

## Pulse radiolysis and laser flash photolysis study of balofloxacin postprint

**Authors:** Yulie Xu, LIU Yancheng, LI Haixia, Peng Zhang, TANG Ruizhi, CAO Xiyan, Wang Wenfeng

**Date:** 2023-06-18T00:00:00+00:00

### Abstract

Pulse radiolysis studies of the reactions between balofloxacin (BFX) and  $e_{aq}^-$ , hydroxyl radical ( $\cdot OH$ ), and  $N_3\cdot$  were carried out to investigate the photosensitive toxicity of BFX. The BFX radical anion formed in the reaction of BFX with  $e_{aq}^-$  was located at 380 nm. The transient species formed in the reaction of BFX with  $\cdot OH$  radical were located in the region of 370 nm to 580 nm, with a maximum  $\lambda_{max}$  at 390 nm. The BFX radical cation was obtained by reacting BFX with  $N_3\cdot$ , and showed an absorption band at around 365 nm. The UV-Vis absorption of the BFX was found to be clearly dependent on pH. The pKa value of BFX was estimated to be  $6.0 \pm 0.2$ . Under neutral conditions, the rate constant of BFX reacting with  $N_3\cdot$  and  $e_{aq}^-$  were determined to be  $1.3 \times 10^{10} \text{ mol}^{-1} \cdot \text{s}^{-1}$  and  $1.4 \times 10^{10} \text{ dm}^3 \cdot \text{mol}^{-1} \cdot \text{s}^{-1}$ , respectively.

### Full Text

### Preamble

Nuclear Science and Techniques 24 (2013) S010312

### Pulse Radiolysis and Laser Flash Photolysis Study of Balofloxacin

XU Yulie<sup>1,2</sup>, LIU Yancheng<sup>1,2</sup>, LI Haixia<sup>1,2</sup>, ZHANG Peng<sup>1</sup>, TANG Ruizhi<sup>1,2</sup>, CAO Xiyan<sup>3</sup>, WENG Feng<sup>1,\*</sup>

<sup>1</sup>Shanghai Institute of Applied Physics, Chinese Academy of Sciences, Shanghai 201800, China

<sup>2</sup>Graduate University of Chinese Academy of Sciences, Beijing 100049, China

<sup>3</sup>School of Chemistry and Chemical Engineering, Hunan University of Science and Technology, Xiangtan 411201, China

## Abstract

Pulse radiolysis studies of the reactions between balofloxacin (BFX) and the hydrated electron ( $e_{aq}^-$ ), hydroxyl radical ( $\cdot\text{OH}$ ), and azide radical ( $\text{N}_3\cdot$ ) were carried out to investigate the photosensitive toxicity of BFX. The BFX radical anion formed in the reaction with  $e_{aq}^-$  exhibited an absorption maximum at 380 nm. The transient species formed in the reaction of BFX with  $\cdot\text{OH}$  radical showed absorption in the region of 370–580 nm, with a maximum at 390 nm. The BFX radical cation was obtained by reacting BFX with  $\text{N}_3\cdot$  and displayed an absorption band around 365 nm. The UV-Vis absorption of BFX was clearly pH-dependent, with a  $\text{p}K_a$  value estimated at  $6.0 \pm 0.2$ . Under neutral conditions, the rate constants for BFX reacting with  $\text{N}_3\cdot$  and  $e_{aq}^-$  were determined to be  $1.3 \times 10^{10} \text{ dm}^3 \cdot \text{mol}^{-1} \cdot \text{s}^{-1}$  and  $1.4 \times 10^{10} \text{ dm}^3 \cdot \text{mol}^{-1} \cdot \text{s}^{-1}$ , respectively.

**Key words:** Balofloxacin, Pulse radiolysis, Laser flash photolysis, Fluoroquinolones

## Introduction

Fluoroquinolones (FQs) are among the most successful classes of antibiotic agents, featuring a broad antibacterial spectrum and potent oral absorption. Their pharmacological action targets bacterial DNA gyrase. Despite their therapeutic importance, FQs exhibit significant side effects, particularly phototoxicity and photocarcinogenic activity, which have attracted considerable research attention. The phototoxicity of FQs arises from transient species formed in neutral aqueous media.

Heterolytic defluorination has been identified as the primary photoprocess for many FQs. This reaction is noteworthy because fluorination is uncommon in fluoroaromatic photochemistry, given the strong aromatic C-F bond (dissociation energy  $\approx 120 \text{ kcal} \cdot \text{mol}^{-1}$ ). Balofloxacin (BFX) is a new fourth-generation fluoroquinolone antibiotic with good tolerability and renal excretion. Previous studies have examined the effects of pH and buffer solution on the photochemical properties of BFX using fluorescence spectrometry.

This study investigates the photochemical and photophysical properties of BFX in aqueous media using UV-Vis spectroscopy, fluorescence measurements, laser flash photolysis, and nanosecond pulse radiolysis techniques. The pulse radiolysis experiments examined reactions of BFX with hydroxyl radical ( $\cdot\text{OH}$ ), azide radical ( $\text{N}_3\cdot$ ), and the hydrated electron ( $e_{aq}^-$ ). Transient absorption spectra and kinetic rate constants were obtained, and the pH dependence of BFX was investigated. Understanding the nature of BFX radicals will enable more effective investigation of photosensitive damage to biological molecules.

## 2.1 Materials

Balofloxacin was purchased from J&K Chemical Ltd and used without further purification. NaOH, HClO<sub>4</sub>, and phosphate (analytical grade reagents) were obtained commercially and used as received. Water was purified through a Millipore Milli-Q system. The pH of solutions was measured using a glass electrode.

## 2.2 Laser Flash Photolysis

Laser flash photolysis experiments were conducted using a neodymium-doped yttrium aluminum garnet (Nd:YAG) laser system. This system featured a Q-switched excitation source with 1 J pulse energy and 12 ns pulse width. Harmonics were separated using a beam splitter. Samples were contained in a quartz cell and replaced after each laser pulse. The analyzing beam was generated by a xenon lamp and passed through the samples at a right angle to the laser beam. Monitoring wavelengths were dispersed by a monochromator and detected by a photomultiplier. The detector was connected to an automatic back-off box that allowed transmittance changes to be observed by feeding back an equal and opposite signal to the detector anode current prior to the laser pulse, thus maintaining the anode current near zero.

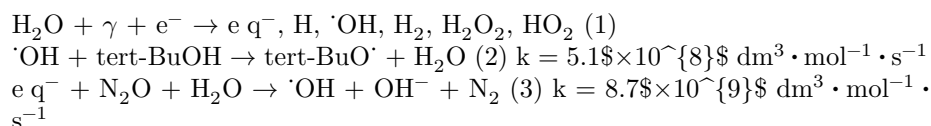
The photomultiplier (Hamamatsu R925) output was displayed on a digitizing oscilloscope. Data were processed on a personal computer using in-house software. Back-off and energy meter readings were digitized using an analogue-to-digital converter connected to a DI-AN data acquisition system. Data were acquired by repeating the above procedure at successive wavelengths.

## 2.3 Pulse Radiolysis

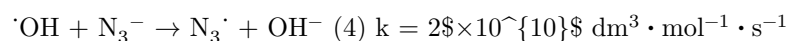
Nanosecond pulse radiolysis experiments were conducted using a 10 MeV linear accelerator that transmitted an electron pulse with 8 ns duration. The dosimetry of the electron pulse was determined using a thiocyanate dosimeter with  $G[(\text{CNS})_2^{\cdot-}] = 5.8$  in  $1 \times 10^{-4}$  mol · dm<sup>-3</sup> KCNS saturated with N<sub>2</sub>O, taking  $\epsilon_{480} = 7600$  dm<sup>3</sup> · mol<sup>-1</sup> · s<sup>-1</sup> for (CNS)<sub>2</sub><sup>·-</sup>. The dose per electron pulse was set at 10 Gy.

A xenon lamp served as the detection light source. The electron pulse and analyzing light beam passed perpendicularly through the quartz cell. The transmitted light entered a monochromator with an R955 photomultiplier. The output signal from the LeCroy WaveMaster 8600A digital oscilloscope was transferred to a personal computer for further analysis.

Tert-butanol was used to scavenge ·OH radicals, creating a reducing environment. Sample solutions were saturated with N<sub>2</sub>O prior to pulse radiolysis to produce an almost uniform ·OH radical oxidizing solution where e q<sup>-</sup> was converted to ·OH based on the following reactions:



To quantitatively produce secondary one-electron oxidants ( $\text{N}_3\cdot$ ), the following reaction was employed. Subsequent reactions of these secondary oxidants with BFX generated one-electron oxidized BFX transient species:



### 3 Results and Discussion

BFX is an effective antibiotic that readily undergoes phototoxicity and photoionization reactions. Investigating the reduction and oxidation products of BFX is therefore necessary for understanding related pathological mechanisms.

#### 3.1 Absorption and Emission Properties

As shown in Fig. 2, the UV-Vis absorption spectrum of BFX exhibits two absorption peaks in the range of 260–400 nm. The short-wavelength absorption band (260–310 nm) primarily arises from  $\pi \rightarrow \pi^*$  electron transitions of the aromatic nucleus, while the long-wavelength absorption band (310–380 nm) originates from  $n \rightarrow \pi^*$  transitions (HOMO-LUMO). As pH increases, the maximum absorption peak shows a blue shift from 293 nm to 285 nm. Simultaneously, the long-wavelength absorption band exhibits a red shift, with absorbance gradually increasing as pH rises. Two clear isosbestic points are observed at 325 nm and 350 nm.

In the pH range of 3–10, the proton equilibrium process of BFX involves only the dissociation of the carboxyl group. Scheme 1 shows four potential proton binding sites in the BFX structure, though this experiment does not identify which specific site is protonated. From these titration curves, a pK value of  $6.0 \pm 0.2$  was deduced for the dissociation of the carboxylic acid group. Thus, at neutral pH, the predominant species is the neutral form.

Figure 3 [Figure 3: see original paper] demonstrates the pronounced effects of pH changes on BFX fluorescence, with maximum fluorescence intensity observed at pH 7.53. The maximum emission wavelength shows a blue shift, and fluorescence intensity gradually increases as pH rises from 2.92 to 7.53. When pH exceeds 7.53, the fluorescence intensity at the maximum emission wavelength decreases with increasing pH. After pH exceeds 12, the fluorescence gradually attenuates and becomes nearly undetectable. The fluorescence spectrum of BFX at pH 7.53 shows a broad band around 460 nm. This shift can be explained by the presence of both an electron-donating amino group and an electron-withdrawing fluorine substituent, which imparts some internal charge transfer character to the  $\pi \rightarrow \pi^*$  excited state. This effect may result from deprotonation of BFX at high pH,

which makes a lone pair of electrons available for intermolecular electron transfer, establishing an efficient pathway for deactivation of the singlet excited state.

### 3.2 Laser Flash Photolysis

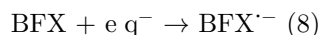
Figure 4 [Figure 4: see original paper] shows the transient absorption spectra obtained via 355 nm laser flash photolysis of BFX ( $1 \times 10^{-4}$  mol  $\cdot$  dm $^{-3}$ ) in aqueous phosphate buffer ( $2 \times 10^{-3}$  mol  $\cdot$  dm $^{-3}$ , pH 7.0) saturated with air, N<sub>2</sub>O, N<sub>2</sub>, and O<sub>2</sub>. By using N<sub>2</sub>O to remove e q $^{-}$  absorption, pure <sup>3</sup>BFX\* absorption can be observed at 720 nm. The transient absorbance of pure e q $^{-}$  can be obtained by subtracting the spectrum obtained in N<sub>2</sub>O-saturated solution from that in N<sub>2</sub>-saturated solution.

As shown in Fig. 5 [Figure 5: see original paper], there is a perfect linear relationship between the quantum yield of hydrated electrons recorded at 720 nm and the laser pulse intensity, indicating that the photoionization of BFX in neutral aqueous solution is a single-photon process, similar to moxifloxacin and ofloxacin. This contrasts with other FQs, whose photoionizations have been found to be biphotonic.

The hydrated electron should react with BFX to form BFX anion radicals. Obvious, relatively long-lived transient absorption is observed at 380 nm, which will be confirmed in the following pulse radiolysis experiments. At 700 nm, as O<sub>2</sub> concentration increases, the absorption peak decreases due to the reaction of e q $^{-}$  with O<sub>2</sub> to produce O<sub>2</sub> $^{\cdot-}$  (Reaction 5). In N<sub>2</sub>O-saturated solution, e q $^{-}$  is scavenged by N<sub>2</sub>O, producing  $\cdot$ OH (Reaction 3). The transient species with characteristic absorption at 360 nm may arise from the BFX radical cation (BFX $^{\cdot+}$ ) formed by reaction with oxidative radicals O<sub>2</sub> $^{\cdot-}$  and  $\cdot$ OH. Intensive photoionization evidently occurs, as confirmed by the formation of hydrated electrons.

#### 3.3.1 Reaction of BFX with e q $^{-}$

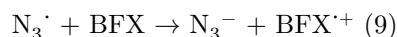
As shown in Fig. 6, a transient absorption spectrum was obtained in the pulse radiolysis of N<sub>2</sub>-saturated neutral aqueous solution containing  $1 \times 10^{-4}$  mol  $\cdot$  dm $^{-3}$  BFX with 0.1 mol  $\cdot$  dm $^{-3}$  tert-butanol added as an  $\cdot$ OH radical scavenger. Under these conditions, hydroxyl radicals are removed by tert-butanol, leaving only e q $^{-}$ . According to Reaction 8, the primary transient product is the BFX anion radical (BFX $^{\cdot-}$ ). The reduction follows pseudo-first-order kinetics, and a rate constant of  $1.4 \times 10^{10}$  dm $^3 \cdot$  mol $^{-1} \cdot$  s $^{-1}$  was obtained at various BFX concentrations.



#### 3.3.2 Oxidation of BFX by N<sub>3</sub> $^{\cdot}$

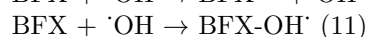
The reactions between the azide radical N<sub>3</sub> $^{\cdot}$  and BFX were studied to investigate the reactions of BFX with  $\cdot$ OH in greater depth, as the latter may involve

complex redox reactions or hydrogen abstraction. In contrast, BFX reacts with  $N_3\cdot$  exclusively via electron transfer to form  $BFX\cdot^+$ . In  $N_2O$ -saturated aqueous solution, hydrated electrons are converted to  $\cdot OH$ , which then oxidizes  $N_3^-$  to form  $N_3\cdot$ . Subsequently, BFX is oxidized by  $N_3\cdot$  through electron transfer. As shown in Fig. 7 [Figure 7: see original paper], the species with maximum absorption at 365 nm is assigned to the BFX radical cation ( $BFX\cdot^+$ ), and the rate constant for Reaction 9 is estimated to be  $1.3 \times 10^{10} \text{ dm}^3 \cdot \text{mol}^{-1} \cdot \text{s}^{-1}$ .



### 3.3.3 Reaction of BFX with $\cdot OH$

Reactions between BFX and  $\cdot OH$  may proceed through multiple pathways: redox reactions producing BFX radical cations, addition reactions forming adducts, and hydrogen abstraction reactions generating BFX neutral radicals (Reactions 10-12). However, the reaction between subsequent BFX products attacked by  $\cdot OH$  and biological materials is complex and requires further investigation.



## 4 Conclusion

This work provides systematic results on the photochemical and photophysical properties of BFX. The  $pK_a$  value was determined to be  $6.0 \pm 0.2$  through UV-Vis spectral analysis. BFX fluorescence showed clear pH dependence, with maximum intensity at pH 7.53. The photochemical and photophysical properties of  $N_3\cdot$  were investigated via pulse radiolysis. Since the biological consequences of reactions between these transient species and biomolecules remain unclear, further exploration is needed to understand the underlying mechanisms.

## References

1. Domagala J M, Hanna L D, Heifetz C L, et al. J Med Chem, 1986, 29: 394-404.
2. Wolfson J S, Hooper D C. Clin Microbiol Rev, 1989, 2: 378-424.
3. Martinez L, Chignell C F. J Photoch Photobio B, 1998, 45: 51-59.
4. Cheng L L, Zhao P, Wang M, et al. Acta Phys-Chim Sin, 2009, 25: 25-29.
5. Lhiaubet-Vallet V, Bosca F, Miranda M A. Photochem Photobiol, 2009, 85: 861-868.

6. Van Doorslaer X, Demeestere K, Heynderickx P M, et al. *Appl Catal B-Env*, 2011, 101: 540-547.
7. Mella M, Fasani E, Albini A. *Helv Chim Acta*, 2001, 84: 2508-2519.
8. Ling X, Zhong W Y, Huang Q, et al. *J Photoch Photobio B*, 2008, 93: 172-176.
9. ElWalily A F M, Belal S F, Bakry R S. *J Pharmaceut Biomed*, 1996, 14: 561-569.
10. Fasani E, Mella M, Caccia D, et al. *Chem Commun*, 1997, 1329-1330.
11. Cuquerella M C, Bosca F, Miranda M A. *J Org Chem*, 2004, 69: 7256-7261.
12. Fasani E, Mella M, Albini A. *Eur J Org Chem*, 2004, 5075-5082.
13. Cuquerella M C, Miranda M A, Bosca F. *J Phys Chem A*, 2006, 110: 2607-2612.
14. Cuquerella M C, Miranda M A, Bosca F. *J Phys Chem B*, 2006, 110: 6441-6443.
15. Fasani E, Monti S, Manet I, et al. *Org Lett*, 2009, 11: 1875-1878.
16. Qi X J, Wang J X, Liu Z R. *Chin J Analyt Chem*, 2006, 34: 1047-1047.
17. Yan Z Y, Shao X F, Jiang X M, et al. *Spectroscopy Spectra Anal*, 2006, 26: 1494-1498.
18. Yao S D, Sheng S G, Cai J H, et al. *Radiat Phys Chem*, 1995, 46: 105-109.
19. Agrawal N, Ray R S, Farooq M, et al. *Photochem Photobiol*, 2007, 83: 1226-1236.
20. Navaratnam S. *J Claridge Photochem Photobiol*, 2000, 72: 283-290.
21. Neugebauer U, Szeghalmi A, Schmitt M, et al. *Spectrochem Acta A*, 2005, 61: 1505-1517.
22. Lorenzo F, Navaratnam S, Edge R, et al. *Photochem Photobiol*, 2009, 85: 886-894.
23. Buxton G V, Greenstock C L, Helman W P, et al. *J Phys Chem Ref*

Data, 1988, 17: 513-886.

24. Lorenzo F, Navaratnam S, R Edge, et al. Photochem Photobiol, 2008, 84: 1118-1125.

25. Lian N, Zhao H C, Sun C Y, et al. Chem J Chin U, 2002, 23: 564-566.

26. Monti S, Sortino S. Photoch Photobio Sci, 2002, 1: 877-881.

*Note: Figure translations are in progress. See original paper for figures.*

*Source: ChinaXiv –Machine translation. Verify with original.*